Original Article

Monte Carlo Simulation for the Radixact™ Tomotherapy Linac Using EGSnrc

Danial Seifi Makrani[1,2], Hassan Ali Nedaei[1,2], Ghazale Geraily[1,2], Alireza Khorami-Moghaddam[3], Nooshin Banaee[4], Hussam Jassim[1,2,5]

[1]Department of Medical Physics and Biomedical Engineering, Tehran University of Medical Sciences, [2]Radiation Oncology Research Centre, Cancer Institute, Tehran University of Medical Sciences, [4]Medical Radiation Research Center, Central Tehran Branch, Islamic Azad University, Tehran, [3]Department of Radiology, Faculty of Allied Medicine, Mazandaran University of Medical Sciences, Sari, Iran, [5]Department of Radiotherapy, Euphrates Cancer Hospital, Kufa, Najaf, Iraq

Abstract

Purpose: When exact information regarding the treatment head and initial electron beam is available, the Monte Carlo (MC) approach can properly simulate any linear accelerator. However, manufacturers seldom offer information such as the incident electron beam's energy, radial intensity (spot size), or angular spread. This research aims to forecast these features and verify an MC-simulated linear accelerator model using measurements. **Materials and Methods:** The BEAMnrc code simulated a 6 MV photon beam from a Radixact™ Tomotherapy Linac. Percentage depth dose and beam profile calculations were conducted using DOSYXZnrc by various electron energies and spot sizes and compared to measurements using a Gamma index with two distinct criterion sets. Furthermore, the fine-tuned electron energy and spot size profiles were created to minimize any disparities using distinct angle spreads. Finally, the output factors (OFs) for various field sizes were compared. **Results:** The MC model's fine-tuned electron energy was determined to be 5.8 MeV, with 88.6% of the calculation points passing the 1%/1 mm γ test. A circular radial intensity of 1.4 mm best represented the 6 MV photon beam regarding spot size. Furthermore, a mean angular spread of 0.05 reduced the disparity in cross-field profile between computation and measurement. The most considerable disparities between the MC model OFs and observations were 1.5%. **Conclusion:** Using the BEAMnrc code, a reliable MC model of the Radixact™ Tomotherapy Linac can be created, as shown in this paper. This model can be used to compute dose distributions with confidence.

Keywords: BEAMnrc, DOSXYZnrc, Monte Carlo, tomotherapy

Received on: 15-02-2024 **Review completed on:** 02-04-2024 **Accepted on:** 14-04-2024 **Published on:** 21-09-2024

Introduction

In the past few years, intensity-modulated radiotherapy (IMRT) has become one of the most important ways to treat tumors. However, radiotherapy with high amounts of radiation can kill cancer cells and shrink the tumor, but if the proper precautions are not taken, it can also do a lot of damage to the organs at risk (OAR) around the tumor.[1-3] Helical tomotherapy (HT) is a sophisticated IMRT delivery technology that also does image-guided adaptive radiotherapy.[2-5] Tomotherapy's distinctive architecture enables it to provide more complicated modulated coplanar beam combinations from a broader range of angles than is generally the case with traditional IMRT.[6,7] The goal of HT is to provide a conformal radiation dose distribution to a planned target volume while avoiding neighboring OAR by using a narrow, intensity-modulated photon fan beam that travels in a helical manner.[8] In order to guarantee the maximum possible protection of the patient, it is critical to estimate the optimum dose for tumor regions and surrounding OAR.[8-12] Characterizing the shape of the radiation equipment's beam is a key part of figuring out the dose in the areas listed. The Monte Carlo (MC) program is thought to be the most accurate way to figure out how doses are distributed in tissues.[13,14] It is appropriate for radiotherapy questions in which charged or uncharged particles interact with a medium and put in motion charged particles that deposit energy along their paths through the medium.[15] Each particle generates an interaction waterfall, and the relevant physical parameters are

Access this article online

Quick Response Code:

Website: www.jmp.org.in

DOI: 10.4103/jmp.jmp_29_24

Address for correspondence: Dr. Hassan Ali Nedaei, Department of Medical Physics and Biomedical Engineering, Tehran University of Medical Sciences, Tehran, Iran. Radiation Oncology Research Centre, Cancer Institute, Tehran University of Medical Sciences, Tehran, Iran. E-mail: nedaieha@tums.ac.ir

How to cite this article: Makrani DS, Nedaei HA, Geraily G, Khorami-Moghaddam A, Banaee N, Jassim H. Monte Carlo simulation for the Radixact™ Tomotherapy Linac using EGSnrc. J Med Phys 2024;49:379-86.

recorded in a phase space.[16] The MC techniques are regarded as the most reliable way for estimating dose distributions for treatment-planning reasons, since the route of a particle is termed history.[17,18]

The commissioning of the model to match the dose data was the initial stage in the MC modeling. In order to characterize the accurate geometry of any radiotherapy equipment, the compositions of the components, as well as the geometrical dimension information, must be well understood. Usually, the manufacturer will supply this data. Mistakes in component materials and compositions, geometrical errors, and energy choice may all increase the uncertainty of dose calculations.[19] However, the manufacturer does not routinely disclose the main details, such as the incidence of electron energy on the target and the generation of bremsstrahlung photons.[20,21] This data also contains the angular divergence of the incoming electron beam on the target and the radial intensity distribution (full width at half maximum [FWHM] or focused spot size). This information may be generally predicted through trial-and-error methods.[22-24] Several papers have investigated the photon beam spot size and primary electron energy in radiation accelerators.[25-27]

In the literature, few authors reported relevant dosimetry data for Tomotherapy. Only in 2023, Quispe-Huillcara *et al*. modeled and characterized the radiation beam of the Radixact tomotherapy equipment using the MC Code MCNP5.[28] However, to our knowledge, there is no study that models and validates the Radixact™ Tomotherapy linac for a 6 MV photon beam using EGSnrc regarding incident electron energy, FWHM, and the output factors (OFs). The EGSnrc MC code has been used in previous works to simulate older generations of tomotherapy units, such as Hi-art, confirming the correctness of the MC model by tweaking the missing parameters mentioned above.[29-31]

The MC simulation was carried out in this study using the BEAMnrc and DOSXYZnrc codes.[32,33] The 1 cm × 40 cm, 2.5 cm × 40 cm, and 5 cm × 40 cm field sizes, with a source-to-axis distance of 85 cm, were studied in a water phantom using DOSXYZnrc to model radiation transport and derive the percentage depth dose (PDD) and beam dose profiles. The Gamma Index (GI) was used in the simulation validation to compare dose distributions quantitatively, following Low *et al*.[34] The focus of this study is to model and validate Radixact™ Tomotherapy linac, which is demonstrated for the first time. In order to determine the precise spot size and angular divergence, the dose profiles and PDDs were compared first to determine the optimum incident electron energy match. Finally, the OFs for various field sizes were compared between the measurements and the fine-tuned MC model.

Materials and Methods

Tomotherapy unit

Figure 1 depicts a schematic representation of a Radixact™ tomotherapy unit with the primary pieces identified.

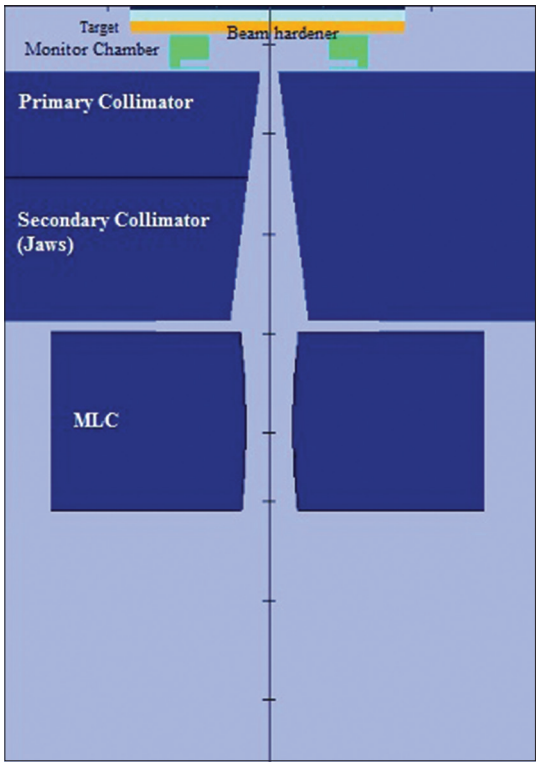

Figure 1: Model of the Radixact™ tomotherapy unit as used in the Monte Carlo simulations. MLC: Multileaf collimator

The simulated model of the Tomotherapy head comprises a target assembly, ionization chamber, primary collimator, moveable jaws, and multileaf collimator (MLC) positioned on a computed tomography (CT) scanner-like gantry, allowing them to work as they constantly spin around the central axis of the bore, while a patient travels down a perpendicular axis. The lack of a flattening filter, a thin target, an electron stopper, a beam hardener, and a compact primary collimator distinguishes the Radixact from other IMRT systems, resulting in a drastically different radiation field than other treatment units. The target closest to the incoming electrons consists of a 0.3 cm thick tungsten layer. A 1-cm thick layer of water allows for target rotation and cooling, while a 1-cm-thick metal coating acts as an electron stopper.[35] There are no air gaps between the layers of the target assembly. The primary collimator, made of tungsten, is 8 cm thick and is placed 8 cm from the bottom of the target assembly. The movable jaws (tungsten) are 23 cm distant from the bottom of the target assembly and are directly near the ends of the main collimator (no air gap).[36] In the manner of a CT scanner, the head may spin continuously and concurrently with the movement of the treatment table (helical delivery). When all of the MLC's leaves are open, the jaws may be configured to create three field widths at the isocenter, 1 cm × 40 cm, 2.5 cm × 40 cm, and 5 cm × 40 cm (source-to-surface distance [SSD] = 85 cm). The Jaws and MLC collimate photons emitted by the Linac. The Jaws collimate the beam longitudinally to form its field width, and the MLC collimates it radially (laterally and vertically). The MLC opens and closes to control the quantity of radiation

going through to the patient at a transverse point corresponding to each leaf and is made up of 32 tungsten leaves spread on each side of the beam (64 total leaves). The Radixact machine's MLC is binary, meaning each leaf may be fully open or entirely closed. The MLC's distal side is 40 cm distant from the source in the z-direction,[36] and each leaf is 10 cm thick (in the beam direction), creating a beamlet that is 6.25 mm wide in the transverse direction (in-slice) and 85 cm from the main target's bottom. The leaves migrate laterally (patient inferior-superior or across-slice). Each leaf measures 2 mm (IEC X) on the LINAC side and 3 mm on the patient side, for a total width of 6.25 mm at the isocenter. The radiation field is fan shaped, with a maximum transverse dimension of 40 cm and a changeable lateral dimension (i.e., slice thickness) of up to 5 cm, as dictated by the jaw opening.

Measurement

The commissioned measured data was used to verify and optimize the MC linac model, including the PDDs, dose profiles, and OFs. This measurement was made using a water tank (PTW, Freiburg, Germany) and a 0.125 cc volume PTW semiflex ionization chamber during the clinical commissioning of the Radixact HT device. The beam profiles were measured in Solid Water slabs using Gafchromic EBT3 films (Ashland ISP, Wayne, NJ, USA). The measured dose distribution's estimated standard error of the mean is <1%. Measurements were acquired on the field of 5 cm × 40 cm.

Monte Carlo simulation

The photon beam from the linac was modeled using the BEAMnrc MC (version 2021) code.[32] In the BEAMnrc user code, source number 19 was utilized; furthermore, there are some component modules (CMs) for considering MLC, JAWS, etc. The SYNCMLCE CM was used to model the MLC in static fields. Two-phase space-scoring planes were used in this work. The first scoring plane was located immediately above the MLC, where we generated Phase-Space-File 1 (PSF1). The second scoring plane (which scored PSF2) was located below the MLC and outside the boundary of the dose-scoring phantom. Most of the simulation parameters were left at their default settings. Various variance reduction techniques were utilized to shorten the simulation duration. To boost the simulation's execution speed, range rejection, bremsstrahlung cross-section enhancement (BCSE), directional bremsstrahlung splitting (DBS), and Russian roulette were utilized. The DBS had a splitting number of 10,000 (NBRSPL) and several splitting field radii depending on field size, with an 85 cm SSD at which the field was defined. The BCSE was employed, with values of 20 and 0 for the enhancement constant (BCSE FACTOR C) and enhancement power (BCSE FACTOR), respectively, and a range rejection of 1 MeV. For all areas of the accelerator head and phantom, we utilized an electron cutoff energy (ECUT) of 0.7 MeV and a photon cutoff energy (PCUT) of 0.01 MeV. The energy thresholds for knock-on electrons (AE) and secondary bremsstrahlung (AP) were likewise 0.7 MeV and 0.01 MeV, respectively. Higher ECUT and PCUT were employed to increase simulation efficiency, and the findings were confirmed using ECUT = 0.512 MeV and PCUT = 0.005 MeV. In all MC simulations, electron range rejection measures were disabled. The water tank phantom was modeled using the DOSXYZnrc code.[33] Source number 9 (BEAM treatment head simulation) was used. The MC water phantom has dimensions of 20.25 cm × 20.25 cm × 35 cm and in general, the voxel dimension was 0.5 cm × 0.5 cm × 0.5 cm in all directions for dose profiles to compare measured dose distributions to the results of MC simulations in longitudinal directions. For the PDDs, the voxel size in the Z-direction was adjusted in the build-up area, starting at 1 cm and decreasing to 0.6 cm centered at 1.1 cm depth, the maximum dose depth. The voxel size in the Z-direction after the build-up area was 0.5 cm. Most simulation parameters in the DOSXYZnrc codes were left at their suggested (default) levels. The photon splitting number (n split) approach was utilized and adjusted to 35 to enhance the DOSXYZnrc computation efficiency while fat photons from DBS were removed. Furthermore, the PRESTA-I algorithm was employed as the boundary-crossing technique for efficiency considerations. The Evaluated Photon Data Library cross-section was utilized to represent the photon cross-section for the same reasons.[32] At least 10^9 source particles, generally recycled ten times for dose calculations, were employed for phase space computation. All simulations were run in open field geometry with an 85 cm surface-to-source distance.

Evaluation of Monte Carlo and measurement results

Percentage depth dose, dose profile, and output factor comparison

The energy of the electron source has a significant impact on photon quality, which may be indicated by the relative dose deposition of the beam at various depths of the homogeneous phantom. As a result, energy modifications may be performed based on the percentile depth dose curve. Based on the above, the no. 19 electron source in the BEAMnrc code was selected, and the FWHM of the Gaussian intensity distribution of the circular beam (spot size) was fixed and set to 0.1 cm in the X and Y directions, and the average angular extent was set to 0 by default. This indicates that the beam is perpendicular to the Z-axis. As a result, any influence noticed on the PDD curves is attributed purely to a change in electron energy. To calculate the best match energy, the simulations were conducted using various monoenergetic energies ranging from 5 MeV to 6 MeV that increased by 200 keV increments. The initial energy was iteratively modified, and the simulations were repeated until the estimated PDD curves aligned with the observed PDD curves at the maximal dose, which is found at a depth of 1.1 cm, using a constant SSD of 85 cm.

Because electron source no. 19 in BEAMnrc has a Gaussian radial distribution, the FWHM of the electron source must also be evaluated after identifying the ideal electron energy match. The FWHM relates to the beam's Gaussian distribution in the Z-direction and has less influence on the PDD but a bigger effect on the dose profiles. The FWHM range tested was from

1 mm to 2 mm in 0.2 mm increments (in both the X and Y axes). The comparison field size was 5 cm × 40 cm, and the SSD was 85 cm. As a result, the PDD curves were utilized to establish the electron mean energy, and the dose profile was evaluated to determine the beam's FWHM.[37] In order to calculate the best match profile, the simulations were conducted using various mean angular divergence ranging from 0.01° to 1.1° that increased by 0.02° increments.

Finally, the OFs of the fine-tuned MC model for various field sizes were computed and compared to the experimental results. Field sizes of 1 cm × 40 cm, 2.5 cm × 40 cm, and 5 cm × 40 cm were included, with a constant SSD of 85 cm. In this work, the OF was defined as the ratio of the dose at a 10 cm depth in a phantom of a specific field size to that of a reference field size, in this instance, 5 cm × 10 cm. For all field sizes, the SSD of 85 cm was maintained constant.

Depth dose

After determining the optimal angle spread, the dose profiles at two depths (5 cm depth and 10 cm depth) with a constant SSD of 85 cm for a 5 cm × 40 cm field size were calculated in a 20.25 cm × 20.25 cm × 35 cm MC water phantom. The z-direction voxel dimension changed with depth. The voxel size in the xy-plane was 0.5 cm × 0.5 cm around the central axis. For all voxels at depth, the statistical uncertainties in the predicted depth doses were ≤0.5% of the local value.

Comparison of simulation and measurement data by Gamma Index

In order to verify the accuracy of the MC model for the Radixact® Tomotherapy linac, the simulated PDD and beam profiles were compared with the actual results. To achieve this objective, the GI (γ) and the corresponding gamma score were calculated using ScanDoseMatch software.[38] The GI analysis evaluated two dose distributions: (1) the reference dose, which is typically regarded as the gold standard, and (2) the evaluated (target) dose, which is assessed. In the benchmarking procedure, the measured data serves as the reference dose distribution, while the MC calculation (PDD and profile dose data) is employed as the assessed dose.

The GI (γ) is defined as the minimum Euclidean distance between reference dose (D_r) and evaluated (or simulated) dose (D_e) in the reference and evaluated dose distributions, respectively.[39] A particular D_e is compared to all D_r and Γ is calculated as follows:

$$\gamma = \min \sqrt{\frac{(D_r - D_e)^2}{\delta D^2} + \frac{(d_r - d_e)^2}{\delta d^2}}$$

where d_r and d_e are the position of the reference and evaluated doses D_r and D_e respectively, and δD (%) and δd (mm) are the percentage dose difference (DD) and distance-to-agreement (DTA), respectively.

This research used the GI with two sets of acceptance criteria: a 2 mm DTA with a 2% DD, (2%/2 mm), as specified by the AAPM-TG 105, and a more accurate 1%/1 mm.[40] If the gamma value is below one at a given location, it indicates that the assessed dosage meets the requirements at that time. Conversely, if the gamma value equals or exceeds 1, it signifies a failure. The gamma score indicates the proportion of points within the profile that were successfully completed. This method has become the gold standard for the comparison between measured and calculated dose distributions.[41]

Results

Determination of initial electron energy

The simulation was started using default parameters for the initial energy. Although the inventors proposed using a monoenergetic primary beam, the predicted results did not align with the data obtained from experiments. PDD curves of measurement and MC simulation for six different incident electron energies (5 MeV, 5.2 MeV, 5.4 MeV, 5.6 MeV, 5.8 MeV, and 6 MeV) are shown in Figure 2. The relative dose was obtained by normalizing the absorbed dose values to a depth of maximum dose for all PDD curves. As shown in Table 1, Just 5.6 MeV and 5.8 MeV energies passed the 2%/2 mm criterion test, with a 100% passing rate. However, when employing the 1%/1 mm set, all of the calculation locations with just

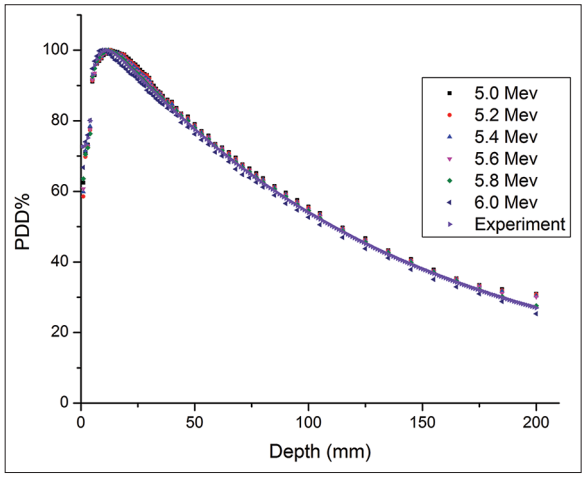

Figure 2: The measured and simulated percentage depth dose curves of the 6 MV photon beam using different electron energies (MeV)

Table 1: Percentage depth dose comparison using a gamma index (γ) with two criteria sets, 2%/2 mm and 1%/1 mm, for various energies (MeV)

Energy (MeV)	2%/2 mm		1%/1 mm	
	GI ≤1%	GI ≤0.5%	GI ≤1%	GI ≤0.5%
5	72.2	35.3	25.6	07.8
5.2	88.6	65.4	36.3	15.4
5.4	93.2	88.6	55.2	32.3
5.6	100	100	80.2	66.2
5.8	100	100	100	88.6
6	76.4	65.2	39.8	23.3

GI: Gamma index

5.8 MeV electron energy passed the test (100% passing rate). Furthermore, 88.6% of the calculation sites for the 5.8 MeV electron energy had values less than 0.5 for the 1%/1 mm set. Figure 3 illustrates the gamma analysis (1%/1 mm) between results of the simulation and experimental for PDD, for the final value of initial energy (5.8 MeV). As shown in Figure 3, the gamma passage rate, represented by the red line, is 100% when there is a 1% DD and a distance of 1 mm. The GI is significantly greater in the buildup region and the tail of the PDD curves, where the PDD values have decreased, compared to the other regions. The observed condition can be elucidated by applying the general law of statistical uncertainty in radiation counting. According to this law, as the number of events decreases, the relative uncertainty of measured and computed counts increases. Consequently, this leads to fluctuations in the GI curve.

Values for full width at half maximum and angular divergence

The simulated dose profiles of a 5 cm × 40 cm field size were compared with measured ones so as to envisage the FWHM values, as FWHM is connected with the spatial distribution of the electron beam hitting the target. This distribution is shaped as the 3D Gaussian. As a result, the 5.8 MeV electron energy was employed to construct dose profiles with varied FWHMs and parallel to the Z-axis, as shown in Figure 4. The dose profiles were created at maximum depth (1.1 cm), corresponding to the maximal dose, and normalized to the central point dose. Based on Table 2, when applying the 2%/2 mm and 1%/1 mm criterion sets, respectively, a circular focus spot with an FWHM of 1.4 mm yielded a flat profile with 98.2% and 87.5% of the calculation points passing the test, and the highest difference was determined to be below 1%. The disparities in the dose profiles grew beyond this FWHM, resulting in the lowest number of points passing the test, i.e., 66.6%, with the 2%/2 mm set for a circular focal spot with an FWHM of 2 mm. As a result, the fine-tuned electron energy of 5.8 MeV and the FWHM of 1.4 mm in both directions were employed to construct dose profiles with mean angular divergences ranging from 0.01° to 1.1° in increments of 0.02° [Figure 5]. This comparison was conducted to reduce the cross-field dose disparities even more for the 5 cm × 40 cm field size. The discrepancies in dose profiles were reduced and marginally lowered with occasional oscillations from 0.01° to 0.05°. Above 0.05°, the discrepancies rose somewhat,

Table 2: Dose profile comparison using gamma index with two criteria sets, the 2%/2 mm and 1%/1 mm, using a circular focal spot with various FWHMs (mm)

FWHM (mm)	2%/2 mm		1%/1 mm	
	GI ≤1%	GI ≤0.5%	GI ≤1%	GI ≤0.5%
1.2	95.5	83.3	83.3	60.6
1.4	98.2	87.5	87.5	77.7
1.6	77.7	62.5	62.5	35.5
1.8	71.4	57.1	57.1	27.5
2	66.6	42.8	42.8	16.6

GI: Gamma index, FWHMS: Full Width of Half Maximum

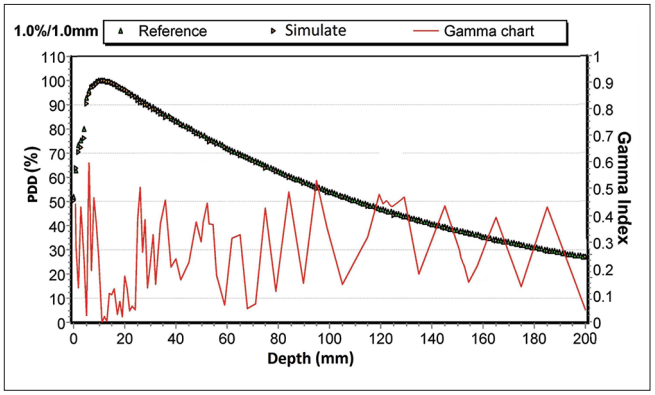

Figure 3: Gamma analysis (1%/1 mm) between results of the simulation and experimental measurements for percentage depth dose for the final value of initial energy (5.8 MeV)

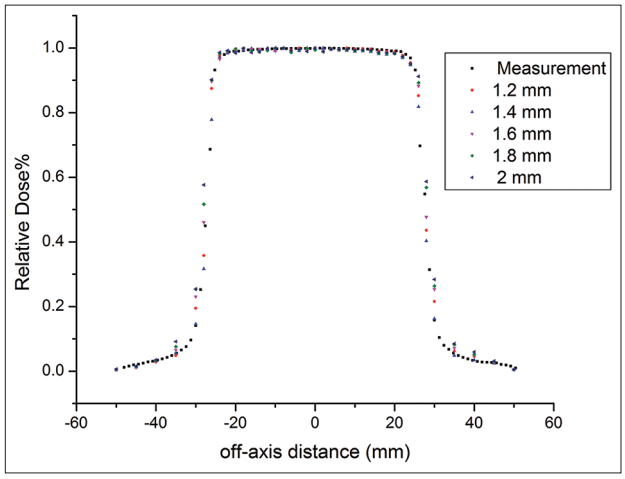

Figure 4: The measured and simulated dose profiles of the 5.8 MeV beam for 5 cm × 40 cm field size at a maximum depth of 1.1 cm using a circular focal spot with various full widths at half maximum values

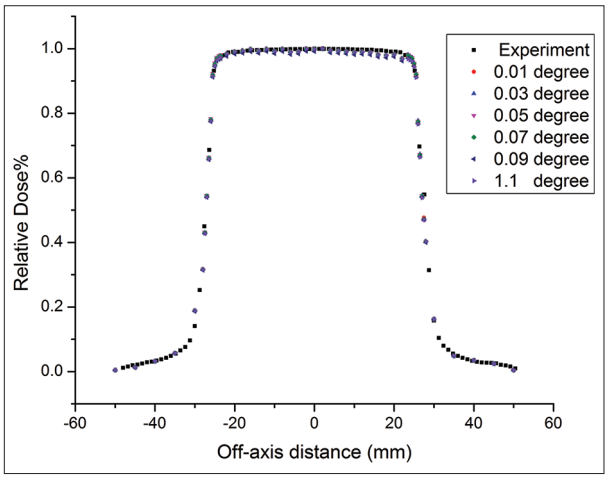

Figure 5: The measured and simulated dose profiles of the 5.8 MeV beam for 5 cm × 40 cm field size at a maximum depth of 1.1 cm with full width at half maximum of 1.4 mm using different mean angular divergences

reaching 62.2% with the 1%/1 mm set when the mean angular divergence was set to 1.1°.

Consequently, as shown in Table 3, the mean angular divergence of 0.05° from the Z-axis reflected the best match with the measurement, with a pass rate of 95.5% when applying the 1%/1 mm set criterion. Figure 6 illustrates the gamma analysis (2%/2 mm and 1%/1 mm) between the results of the simulation and experimental dose profile for the final value of initial energy (5.8 MeV), FWHM (1.4 mm) and mean angular spread (0.05°). Additionally, the dose profiles at different depths for a 5 cm × 40 cm field size of the MC model, with a circular focal spot with FWHM of 1.1 cm and an angular divergence of 0.05°, were generated and compared with the measurements with γ index using the 2%/2 mm set criteria, as shown in Figure 7. Gamma analysis (1%/1 mm) between results of the simulation and experimental measurements for normalized profile, for 5 cm depth and 10 cm depth are presented in Figure 8.

Output factor comparison

Finally, the OFs for various field sizes were calculated using the fine-tuned MC model, with an electron energy of 5.8 MeV and a circular focus point with an FWHM of 1.4 mm and a mean angular divergence of 0.05. Table 4 displays the differences in OF and MC for various field sizes. The lowest variance was around 0.54% for the 2.5 cm × 40 cm field size, while the highest difference was approximately 1.5% for the 1 cm × 40 cm field size. As a consequence, the MC model produced excellent agreement with the data.

Discussion

The determination of the initial electron parameters is an important part of simulating radiation transfer using MC methods. The lack of detailed knowledge of initial electron beam parameters, in the MC simulation of linear accelerator photon beams, has led many researchers to use various methods to estimate them. The mean energy and FWHM of the incident electron beam are usually adjusted by a trial and error method, to match the calculated and experimental data. In the current work, the influence of the mean electron energy, FWHM and mean angular divergence of incident electron beam on the absorbed dose distribution in water was investigated. The dosimetric effects of the above parameters were studied using depth-dose and dose-profile curves. The above settings secure that our results have been relieved from fluctuations associated with electron contamination and statistical noise around depth of maximum. The initial parameters give some parameters of exit beam which include real mean energy and FWHM of beam. For Radixact X9 tomotherapy system, PDD curves were obtained from MC simulation at the field size of 5 cm × 40 cm with initial electron energy of 5, 5.2, 5.4, 5.6, 5.8 and 6 MeV with FWHM of 1.2, 1.4, 1.6, 1.8 and 2 mm. According to Sheikh-Bagheri and Rogers,[42] the PDD curves exhibit sensitivity to changes in mean energy, while the lateral beam dose curves demonstrate sensitivity to both mean energy and FWHM. Our results indicate that with the incident electron energy of 5.8 MeV, Gaussian distribution with FHWM of 1.4 mm, and mean angular divergences of 0.05°, the resulting DDs with respect to measurements will be lower than 1%. The selection of 1% as the maximum difference between the calculated and measured dose has been decided, having in mind the 2% as the maximum error in dose calculation, proposed by ICRU. Several factors may contribute to the above error of 2%, such as the simulation

Table 3: Gamma index for dose profile at the maximum depth dose for different mean angular spreads using two criteria

Mean angular divergence (°)	2%/2 mm		1%/1 mm	
	GI ≤1%	GI ≤0.5%	GI ≤1%	GI ≤0.5%
0.01	98.2	87.5	87.5	75
0.03	95.5	83.3	83.3	73.3
0.05	100	100	95.5	77.7
0.07	95.5	93.3	93.3	75
0.09	95.5	82.2	82.2	66.6
1.1	93.3	77.7	77.7	62.2

GI: Gamma index

Table 4: Output factor differences between the measurements and fine-tuned Monte Carlo model for different field sizes

Field size (cm²)	Measurement	MC	Difference (%)
1×40	0.787	0.799	1.5
2.5×40	0.896	0.902	0.54
5×40	1.025	1.033	0.77

MC: Monte Carlo

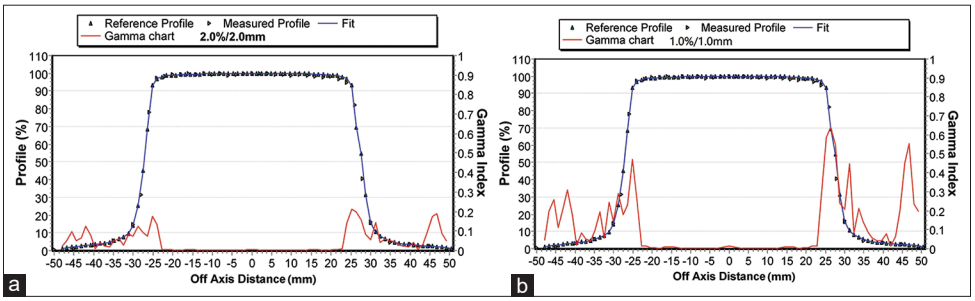

Figure 6: Gamma analysis between results of the simulation and experimental measurements for profile, for the final value of initial energy (5.8 MeV), full width at half maximum (1.4 mm) and mean angular spread (0.05°), (a) with 2%/2 mm and (b) with 1%/1 mm)

of the radiation source, the dosimetric effects of the CT number to density conversion, the density-to-material conversion, and the dose-to-material to dose-to-water conversion. In our study, only the radiation source modeling was examined. Therefore, our decision to select 1% as the maximum error may be considered prudent. An exact comparison of the results of this work with previous works is not possible because it is the first time that Radixact X9 tomotherapy linac has been simulated, however in the studies that simulated the first type of HT, Jeraj *et al*. obtained the best fit experimental values with incident electron energy of 5.7 MeV and the radial dependence of the incident electron beam was Gaussian with the FWHM of 1.4 mm.[29] Sterpin *et al*. found a monoenergetic electron source with an energy of 5.5 MeV and a spatial Gaussian distribution with FHWM of 1.4 mm for benchmarking the simulation with measurements.[30] Hsiao *et al*. found that the incident electron energies had Gaussian (normal) distribution with a mean of 5.0 MeV and a standard deviation of 0.5 MeV.[43] Quispe *et al*. simulated tomotherapy linac with MCNP5 code and their results consisted of an electron source that emits Gaussian distribution particles with an average energy of 5.7 MeV and a standard deviation of 0.3 MeV.[28]

Comparing the measured results and the MC results point by point revealed that 100% points of MC PDD curve (with initial electron energy of 5.8 MeV) and 95.5% points of MC lateral profile (with incident electron energy of 5.8 MeV, FHWM of 1.4 mm, and mean angular divergences of 0.05 °) agree with the measurement using 1%/l mm acceptance criteria. The disparities observed in the buildup region and the tail of the PDD curves can be attributed to the general law of statistical uncertainty in radiation counting. Additionally, there are fluctuations at the edge of the profile curve (penumbra region), where the doses are very low, resulting in a difference between the calculated and measured doses. Similar findings were documented in the study conducted by Tai *et al*.[24] Also, the beam profile is compared with MC results at depths of 1.1 cm (maximum depth), 5 cm, and 10 cm. The FWHM of all the profiles of different depths agrees with the measurements to within 1%1 mm criteria. This indicates the jaws and the MLC have correctly defined geometries.

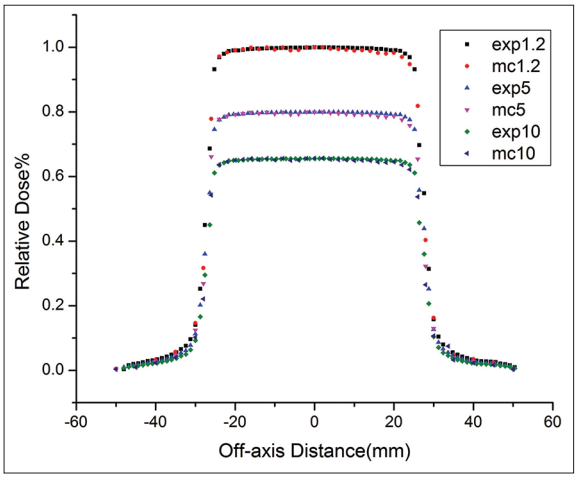

Figure 7: The measured and simulated dose profiles of the 5.8 MeV beam with full width at half maximum of 1.4 mm using 0.05° mean angular divergences for 5 cm × 40 cm field size at different depths

Conclusion

A comprehensive simulation of the treatment head can offer precise information regarding the incident beam on the patient, which is essential for intricate planning purposes. Furthermore, the utilization of the treatment head model has the potential to enhance comprehension of clinical beam features, facilitate the design of accelerator and beam models, and enhance the precision of clinical dosimetry through the provision of more authentic data.

In this current work, the head of Radixact X9 tomotherapy accelerator for a configuration of 5cm × 40 cm field size has been modeled and the three parameters of the initial electron beam have been investigated to validate BEAMnrc model, as they represent the major characteristics of incident beam on the target. Dose distributions (beam profile and PDD) have been calculated in a homogenous water phantom using DOSXYZnrc user code. A good agreement between measured and calculated dose was obtained when the mean energy, mean angular spread, and spot size were 5.8 MeV, 0.05° from the Z-axis, and 1.4 mm, respectively. Correspondingly, the model was accurate between 0.28% and 1.5% in the OF comparison. Ultimately, this MC code simulation using the described methodology can reproduce a known result. So, this work sets the stage for future work that will use the Radixact X9 tomotherapy accelerator MC model to check the results of TPS calculations in situations

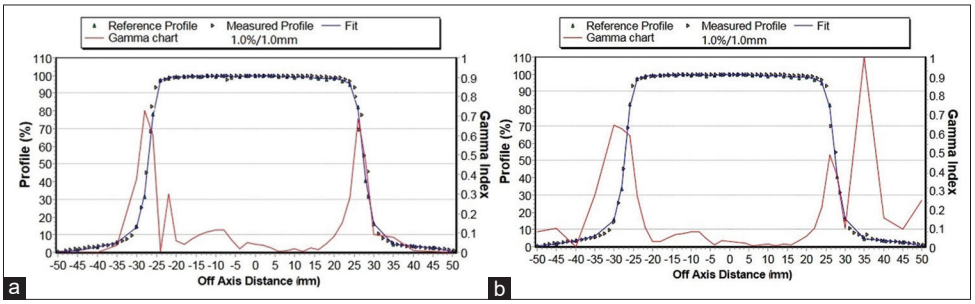

Figure 8: Gamma analysis (1%/1 mm) between results of the simulation and experimental measurements for normalized profile, for (a) 5 cm depth and (b) 10 cm depth

where the MC method is known to give a better understanding of dose distributions, such as when there are large differences in density levels or dose in build-up regions. Additionally, it can improve the comprehension of clinical beam features and enhance the precision of clinical dosimetry through the provision of more authentic fluence data.

Financial support and sponsorship

Nil.

Conflicts of interest

There are no conflicts of interest.

References

1. Yartsev S, Kron T, Van Dyk J. Tomotherapy as a tool in image-guided radiation therapy (IGRT): Theoretical and technological aspects. Biomed Imaging Interv J 2007;3:e16.
2. Beavis AW. Is tomotherapy the future of IMRT? Br J Radiol 2004;77:285-95.
3. Mackie TR, Balog J, Ruchala K, Shepard D, Aldridge S, Fitchard E, *et al*., editors. Tomotherapy. In: Seminars in Radiation Oncology. Semin Radiat Oncol: Elsevier; 1999.
4. Yan D. Image-guided/adaptive radiotherapy. In: New Technologies in Radiation Oncology. 2006. p. 321-36.
5. Kupelian P, Langen K. Helical tomotherapy: Image-guided and adaptive radiotherapy. Front Radiat Ther Oncol 2011;43:165-80.
6. Mackie TR. History of tomotherapy. Phys Med Biol 2006;51:R427-53.
7. Kissick MW, Fenwick J, James JA, Jeraj R, Kapatoes JM, Keller H, *et al.* The helical tomotherapy thread effect. Med Phys 2005;32:1414-23.
8. Mackie TR. From model-based dose computation to tomotherapy. Med Phys 2023;50 Suppl 1:70-3.
9. Chen Q, Lu W, Chen Y, Chen M, Henderson D, Sterpin E. Validation of GPU based tomotherapy dose calculation engine. Med Phys 2012;39:1877-86.
10. Gibbons JP, Smith K, Cheek D, Rosen I. Independent calculation of dose from a helical tomotherapy unit. J Appl Clin Med Phys 2009;10:103-19.
11. Kosaka T, Takatsu J, Inoue T, Hara N, Mitsuhashi T, Suzuki M, *et al.* Effective clinical applications of Monte Carlo-based independent secondary dose verification software for helical tomotherapy. Phys Med 2022;104:112-22.
12. Kodama T, Saito Y, Hatanaka S, Hariu M, Shimbo M, Takahashi T. Commissioning of the Mobius3D independent dose verification system for tomotherapy. J Appl Clin Med Phys 2019;20:12-20.
13. Can S, Harmankaya İ, Atilla Ö, Balkanay AY, Karaçetin DJ, Journal SM. Monte Carlo-based volumetric arc radiation therapy versus helical tomotherapy in terms of tumor control probability and normal tissue complication probability for endometrial cancers. Cam Sakura Med J 2021;1:28-36.
14. Schubert K, Wester X, Weinmann C, Erdem S, Oetzel D, Debus J. Commissioning of tomotherapy treatment planning in RayStation. Radiother Oncol 2020;152:S748-S749.
15. Verhaegen F, Seuntjens J. Monte Carlo modelling of external radiotherapy photon beams. Phys Med Biol 2003;48:R107-64.
16. Andreo P. Monte Carlo simulations in radiotherapy dosimetry. J Radiat Oncol 2018;13:1-15.
17. Rogers DJ. Monte Carlo techniques in radiotherapy. Phys. Canada 2002;58:63-70.
18. El Naqa I, Pater P, Seuntjens J. Monte Carlo role in radiobiological modelling of radiotherapy outcomes. Phys Med Biol 2012;57:R75-97.
19. Spezi E, Lewis G. An overview of Monte Carlo treatment planning for radiotherapy. Radiat Prot Dosimetry 2008;131:123-9.
20. Makrani DS, Hasanzadeh H, Pourfallah TA, Ghasemi A, Jadidi M, Babapour H, *et al*. Determination of primary electron beam parameters in a Siemens primus linac using Monte Carlo simulation. Archives of Advances in Biosciences 2015;6:75-79.
21. Junior JR, Salmon H, Menezes A, Pavan G, Rosa L, Silva AJ. Simulation of Siemens ONCOR™ expression linear accelerator using phase space in the MCNPX code. Progress in Nuclear Energy 2014;70:64-70.
22. Bhagroo S, French SB, Mathews JA, Nazareth DP. Secondary monitor unit calculations for VMAT using parallelized Monte Carlo simulations. J Appl Clin Med Phys 2019;20:60-9.
23. Ohira S, Takegawa H, Miyazaki M, Koizumi M, Teshima T. Monte Carlo modeling of the agility MLC for IMRT and VMAT calculations. *In Vivo* 2020;34:2371-80.
24. Tai DT, Son ND, Loan TT, Tuan HD. A method for determination of parameters of the initial electron beam hitting the target in linac. J Phys Conf Ser 2017;851:12-32.
25. Li Y, Sun X, Liang Y, Hu Y, Liu C. Monte Carlo simulation of linac using PRIMO. Radiat Oncol 2022;17:185.
26. Tuğrul T, Eroğul O. Determination of initial electron parameters by means of Monte Carlo simulations for the Siemens artiste linac 6 MV photon beam. Rep Pract Oncol Radiother 2019;24:331-7.
27. Pourfallah T, Seyed Abousaeedi M, Seifi Makrani D, Mihandoust E, Davoudian S. Evaluation of lung dose in esophageal cancer radiotherapy using Monte Carlo simulation. J Mazandaran Univ Med Sci 2020;29:41-9.
28. Quispe-Huillcara B, de-la-Rosa KM, Reyes U, Cerón PV, Vega HR, Sosa MA. Characterization of the radiation beam of a tomotherapy equipment with MCNP. Appl Radiat Isot 2023;200:110978.
29. Jeraj R, Mackie TR, Balog J, Olivera G, Pearson D, Kapatoes J, *et al.* Radiation characteristics of helical tomotherapy. Med Phys 2004;31:396-404.
30. Sterpin E, Salvat F, Cravens R, Ruchala K, Olivera GH, Vynckier S. Monte Carlo simulation of helical tomotherapy with PENELOPE. Phys Med Biol 2008;53:2161-80.
31. Zhao YL, Mackenzie M, Kirkby C, Fallone BG. Monte Carlo calculation of helical tomotherapy dose delivery. Med Phys 2008;35:3491-500.
32. Rogers D, Walters B, Kawrakow IJ. BEAMnrc users manual. Nrc Report Pirs 2009;509:12.
33. Walters B, Kawrakow I, Rogers DJ. DOSXYZnrc users manual. Nrc Report Pirs 2005;794:57-8.
34. Low DA, Harms WB, Mutic S, Purdy JA. A technique for the quantitative evaluation of dose distributions. Med Phys 1998;25:656-61.
35. Ruchala KJ, Olivera GH, Schloesser EA, Mackie TR. Megavoltage CT on a tomotherapy system. Phys Med Biol 1999;44:2597-621.
36. Incorporated A. Radixact® Physics Essentials Guide; 2017. p. 1-618.
37. Almberg SS, Frengen J, Kylling A, Lindmo T. Monte Carlo linear accelerator simulation of megavoltage photon beams: Independent determination of initial beam parameters. Med Phys 2012;39:40-7.
38. Official Website of ScanDoseMatch. Available from: https://www.qxrayconsulting.com/sdm/.
39. Low DA. Gamma dose distribution evaluation tool. J Phys Conf Ser 2010;250:65-71.
40. Chetty IJ, Curran B, Cygler JE, DeMarco JJ, Ezzell G, Faddegon BA, *et al.* Report of the AAPM task group no. 105: Issues associated with clinical implementation of Monte Carlo-based photon and electron external beam treatment planning. Med Phys 2007;34:4818-53.
41. Hussein M, Rowshanfarzad P, Ebert MA, Nisbet A, Clark CH. A comparison of the gamma index analysis in various commercial IMRT/VMAT QA systems. Radiother Oncol 2013;109:370-6.
42. Sheikh-Bagheri D, Rogers DW. Sensitivity of megavoltage photon beam Monte Carlo simulations to electron beam and other parameters. Med Phys 2002;29:379-90.
43. Hsiao Y, Stewart RD, Li XA. A Monte-Carlo derived dual-source model for helical tomotherapy treatment planning. Technol Cancer Res Treat 2008;7:141-7.